Elsevier Editorial System(tm) for General and Comparative Endocrinology
Manuscript Draft

Manuscript Number:

Title: The C-terminal domains of melanocortin-2 receptor (MC2R) accessory proteins (MRAP1) influence their localization and ACTH-induced cAMP production.

Article Type: Regular Article

Keywords: MRAP; MC2R; ACTH; MRAP localization; MRAP expression; cAMP

Corresponding Author: Professor Nicole Gallo-Payet, PhD

Corresponding Author's Institution: Facuté of Medicine, University of Sherbrooke

First Author: Nicole Gallo-Payet, PhD

Order of Authors: Nicole Gallo-Payet, PhD; Simon Roy, PhD; Sébastien J Roy, MSc; Sandra Pinard, BSC; Maria Josep Agulleiro, PhD; Jose Miguel Cerda-Reverter, PhD; Jean-Luc Parent, PhD

Abstract: ACTH binding to the human melanocortin-2 receptor (MC2R) requires the presence of the MC2R accessory protein1 isoform, MRAP□ or MRAP□. This study evaluated the role of the isoform-specific C-terminal domains of MRAP with regard to their cellular localization, topology, interaction with MRAP2 and cAMP production. When stably expressed in HEK293/FRT cells or in B16-G4F mouse melanoma cells (an MSH receptor-deficient cell clone), MRAP□ and MRAPdCT (truncated MRAP1, N-terminal only) localized mainly around the nuclear envelope and within dense intracellular endosomes, while MRAP□ exhibited a strong localization at the plasma membrane, and partially with rapid recycling endosomes. MRAP□ and MRAPdCT both exhibited dual-topology (Ncyto/Cexo and Nexo/Ccyto) at the plasma membrane whereas MRAP□ exhibited only Ncyto/Cexo topology at the plasma membrane while adopting dual-topology in intracellular compartments. Both MRAP□ and MRAP2 colocalized in intracellular compartments, as opposed to weak colocalization between MRAP□ and MRAP2. MRAP2 and MC2R enhanced the expression of MRAP1 isoforms and vice versa. Moreover, in both HEK293/FRT and B16-G4F cells, ACTH failed to activate MC2R unless MRAP1 was present. MRAP1 expression enhanced MC2R cell-surface expression as well as concentration-dependent cAMP accumulation. In the presence of human or zebrafish MC2R, MRAP□ induced the highest cAMP accumulation while MRAPdCT induced the lowest. Together, the present findings indicate that the C-terminal domains of MRAP dictate their intracellular localization in addition to regulating ACTH-induced cAMP production. These preferential localizations suggest that MRAP□ is involved in MC2R targeting to the plasma membrane, while MRAPβ may enhance ACTH-MC2R coupling to cAMP production.

Suggested Reviewers: Akiyoshi Takahashi PhD
Professor, School of Marine Biosciences, Kitasato University
akiyoshi@kitasato-u.ac.jp
Except in melanocortins

Opposed Reviewers: Adrian J Clark MD, PhD
Professor, School of Medicine and Dentistry, , University of London, UK
a.j.clark@qmul.ac.uk

a competitor working exactly in the same field

Patricia M Hinkle PhD
Professor, Department of Pharmacology and Physiology , University of Rochester
patricia_hinkle@urmc.rochester.edu
a competitor working exactly in the same field

December 29th, 2011

Doctor Robert Dores
Editor-in-chief,
General and Comparative Endocrinology

Dear Dr. Dores :
Please find enclosed a manuscript entitled " The C-terminal domains of melanocortin-2 receptor (MC2R) accessory proteins 1 (MRAP1) influence their localization and ACTH-induced cAMP production" by Simon Roy, Sébastien J. Roy, Sandra Pinard, Maria Josep Agulleiro, José Miguel Cerdá-Reverter, Jean-Luc Parent and myself for publication in General and Comparative Endocrinology.

As indicated in the highlight bullets, when stably expressed in 293/FRT cells or in the B16-G4F-MC1R-deficient cells, we found that MRAPα was localized around the nuclear envelope and intracellular endosomes while MRAPβ exhibited a strong localization at the plasma membrane. In addition, MRAPα and MRAP2 both colocalized in intracellular compartments whereas MRAPβ and MRAP2 were poorly colocalized and, finally, MRAP2 and MC2R enhanced the expression of MRAP1 isoforms and *vice versa.* We believe our work to be original, not previously performed, and representing an extension of our previous publications (Mol. Endoc, 2007 and 2011) as well as those recently published in the field.

I will not hide the fact that this is the third attempt for submission of this work. Each time, reviewers find the work interesting, well conducted, with one or two reviewers having constructive comments for which we were able to provide quite satisfactory answers. However, in each instance, one particular reviewer (probably always the same) had very pernicious comments, and each time our answers appeared unsatisfactory to warrant publication.

In this new version, we have carefully read all of the comments received before submitting this version. Whenever possible and to the best of our abilities, we have tried to provide all the necessary results to circumvent the criticisms previously raised.

This paper has 10 figures and no supplemental material.

I certify that this manuscript represents new, original data, not submitted elsewhere for publication. We hope that our paper will meet the fulfillments for publication in Molecular and Cellular Endocrinology.

Since you are yourself a specialist in the field, we would greatly appreciate your evaluation of our work and you are probably in the best position to choose the appropriate reviewers. We however would like to suggest two names, Akiyoshi Takahashi (from Kitasato University, School of Marine Biosciences, Japan) and Helgi Schiöth **(**Uppsala University, Sweden). We would like to mention that some colleagues are working exactly in the same field. We would appreciate if the paper was not forwarded for review to Dr Adrian J Clark (London, UK) and Patricia Hinke (Rochester, Hinkle) and, in addition, not to José Carlos Garcìa-Borròn (University of Murcia, Spain)

Thank you very much for your kind attention.
Respectfully,
Nicole Gallo-Payet

Suggested reviewers :

Prof. Akiyoshi Takahashi
Kitasato University, School of Marine Biosciences
1-15-1 Kitasato, Minami-ku, Sagamihara, Kanagawa 252-0373, Japan
TEL: +81-42-778-7905
FAX: +81-42-778-5010
EMAIL: **akiyoshi@kitasato-u.ac.jp**

Prof. Helgi Schiöth
Uppsala University
Dept of Neuroscience
Box 593
s-751 24 Uppsala, Sweden
Phone: + 46 18 4714160
Fax: +46 18 511540
Helgi.Schith@neuro.uu.se

Highlights

- MRAPα is localized around the nuclear membrane and intracellular endosomes
- MRAPβ exhibits a strong localization at the plasma membrane
- MRAPα and MRAP2 both colocalize in intracellular compartments
- MRAPβ and MRAP2 are poorly colocalized
- MRAP2 and MC2R enhance the expression of MRAP1 isoforms and *vice versa*

December 29th, 2011

The C-terminal domains of melanocortin-2 receptor (MC2R) accessory proteins (MRAP1) influence their localization and ACTH-induced cAMP production.

Simon Roy[a], Sébastien J. Roy[b], Sandra Pinard[a], Maria Josep Agulleiro[c], José Miguel Cerdá-Reverter[c], Jean-Luc Parent[b] and Nicole Gallo-Payet[a*]

From Service d'Endocrinologie[a], Service de Rhumatologie[b], Département de Médecine, Faculté de Médecine et des Sciences de la Santé, Université de Sherbrooke, Sherbrooke, Québec, Canada[a,b], J1H 5N4 and Department of Fish Physiology and Biotechnology, Instituto de Acuicultura de Torre de la Sal, CSIC, Ribera de Cabanes, Castellón, Spain[c].

Running title: Role of MRAP1 C-terminus in MC2R expression and function

*Corresponding author: Dr. Nicole Gallo-Payet, Service d'Endocrinologie, Département de Médecine, Faculté de Médecine et des Sciences de la Santé, Université de Sherbrooke, 3001, 12e Ave Nord, Sherbrooke, Québec, Canada J1H 5N4.
Tel: 819-564-5243; Fax: 819-564-5292;
Email address: Nicole.Gallo-Payet@USherbrooke.ca

Abbreviations: dCT, deleted C-terminus; DPI, protein disulfide isomerase; ER, endoplasmic reticulum; FRT, Flp recombinase target; FSK, forskolin, a direct activator of adenylyl cyclases; GPCR, G protein-coupled receptor; HEK 293, human embryonic kidney; HRP, horseradish peroxidase; hMC2R, human MC2R; IBMX, 3-isobutyl-1-methylxanthine; MCR, melanocortin receptor; MC1R, melanocortin-1, MSH receptor; MC2R, melanocortin-2 receptor; MRAP, MC2R accessory protein; MSH, Melanocyte-stimulating hormone; NDP-MSH, a potent Nle4,DPhe7-α-MSH analogue; N_{exo}/C_{cyto}, N-terminus at the cytoplasmic side; C-terminus at the exoplasm side; WB, Western blot; 293/FRT, HEK 293 cell line with single genome-integrated FRT site; zf, zebrafish.

Abstract

ACTH binding to the human melanocortin-2 receptor (MC2R) requires the presence of the MC2R accessory protein1 isoform, MRAPα or MRAPβ. This study evaluated the role of the isoform-specific C-terminal domains of MRAP with regard to their cellular localization, topology, interaction with MRAP2 and cAMP production. When stably expressed in HEK293/FRT cells or in B16-G4F mouse melanoma cells (an MSH receptor-deficient cell clone), MRAPα and MRAPdCT (truncated MRAP1, N-terminal only) localized mainly around the nuclear envelope and within dense intracellular endosomes, while MRAPβ exhibited a strong localization at the plasma membrane, and partially with rapid recycling endosomes. MRAPβ and MRAPdCT both exhibited dual-topology (N_{cyto}/C_{exo} and N_{exo}/C_{cyto}) at the plasma membrane whereas MRAPα exhibited only N_{cyto}/C_{exo} topology at the plasma membrane while adopting dual-topology in intracellular compartments. Both MRAPα and MRAP2 colocalized in intracellular compartments, as opposed to weak colocalization between MRAPβ and MRAP2. MRAP2 and MC2R enhanced the expression of MRAP1 isoforms and *vice versa*. Moreover, in both HEK293/FRT and B16-G4F cells, ACTH failed to activate MC2R unless MRAP1 was present. MRAP1 expression enhanced MC2R cell-surface expression as well as concentration-dependent cAMP accumulation. In the presence of human or zebrafish MC2R, MRAPβ induced the highest cAMP accumulation while MRAPdCT induced the lowest. Together, the present findings indicate that the C-terminal domains of MRAP dictate their intracellular localization in addition to regulating ACTH-induced cAMP production. These preferential localizations suggest that MRAPα is involved in MC2R targeting to the plasma membrane, while MRAPβ may enhance ACTH-MC2R coupling to cAMP production.

Keywords: MRAP; MC2R; ACTH; MRAP localization; MRAP expression; cAMP

1. Introduction

Adrenocorticotropic hormone (ACTH) is the major stimulus of the adrenal cortex, having acute and chronic effects on both steroidogenic and trophic action [1-3]. The effects of ACTH are mediated through its receptor called melanocortin-2 receptor (MC2R) [4]. As in the case of all known melanocortin receptors, MC2R is coupled to cAMP production as its main second messenger [5]. MC2R requires the presence of MC2R accessory proteins (MRAPs) for its functional expression [6-8]. MRAP1s are involved in trafficking and signaling of MC2R, while MRAP2s appear essentially involved in MC2R trafficking to the plasma membrane [9-12]. As recently reviewed [13-15], MRAPs are single-passing membrane proteins first identified in adipocytes following differentiation of mouse 3T3-L1 fibroblasts [16]. MRAPs have been found to be essential for ACTH signaling since some patients with an intact MC2R, but a mutated MRAP gene, exhibit familial glucocorticoid deficiency [6, 17]. To date, two types of MRAPs have been identified, namely MRAP (MRAP1) and MRAP2. Humans possess two MRAP1 isoforms (MRAPα and MRAPβ) and one MRAP2, whereas zebrafish express only one MRAP1 (zfMRAP1) and two different MRAP2s (zfMRAP2a and zfMRAP2b) [10] (for review, see [17-19]. Current knowledge indicates that both human MRAP1 isoforms share the same N-terminus and transmembrane domain, while most of their C-terminal domains arise from the alternative splicing of MRAP transcripts [6, 13, 17, 18]. Orthologs of MRAP1 have a strong amino acid identity in their N-terminal domains while their C-termini are completely species- or isoform-specific [10].

MRAPs have an unusual membrane-spanning topology. MRAPα adopts a type II topology in cell-surface enzyme-linked immunoassays (ELISA), as opposed to MRAPβ which exhibits both N_{exo}/C_{cyto} (type I) and N_{cyto}/C_{exo} (type II) topologies [7], as the mouse MRAP1 [8, 9]. Human MRAP1 isoforms confer different functional properties to MC2R [7]. When expressed in the HEK 293/FRT cell line, binding capacity of ACTH to MC2R and maximal cAMP response are higher in the presence of MRAPβ than with MRAPα. In opposition, ACTH potency is increased with MRAPα compared to MRAPβ [7, 11]. One question arising from these observations is the nature of the relationship between the structure of MRAPs and their intracellular trafficking and functions. We emitted the hypothesis that the isoform-specific

structure of the C-terminal domain is involved in specific intracellular localization and association with MC2R, thus dictating its targeting and functional expression. The purpose of the present study was hence to investigate the role of the C-terminal domains of MRAP proteins with regard to their cellular localization, membrane-spanning topology and function with MC2R. To achieve this goal, we constructed a truncated version of MRAP1 named MRAPdCT, which includes only the conserved functional domain between human MRAP1 isoforms (amino acids 1 to 68). In addition, in order to verify the role of the C-terminal domain, cells were transfected with zfMRAP1, in which the C-terminal domain is completely different in terms of sequence from the human MRAP1 isoforms. These constructs were assayed in two cell models, namely HEK 293/FRT cells and B16-G4F mouse melanoma cells. As previously published, the MC2R-expressing HEK 293/FRT or CHO cells represent a useful model for studying ACTH signaling because all MRAP protein isoforms can be expressed in these cells [7, 10, 11, 20]. In addition, this model reproduces concentration-response curves of ACTH-induced cAMP production similarly to those obtained in primary cultures of human and rat adrenocortical cells [21, 22]. On the other hand, the B16-G4F mouse melanoma cells are characterized by the absence of functional MSH receptors (melanocortin-1 receptor, MC1R), while also binding ACTH [23], therefore providing an ideal cell model for comparison with heterologous expression of 293/FRT cells.

2. Materials and Methods

2.1. Materials

Human MC2R cDNA was provided by Dr. Roger D. Cone (Vollum Institute, Oregon Health and Science University, Portland, Oregon). High glucose DMEM (Dulbecco's Modified Eagle's Medium) and Hygromycin B were from Wisent (St-Jean-Baptiste, QC, Canada). FBS (Fetal Bovine Serum), GlutaMAX and Zeocin were from Invitrogen (Burlington, ON, Canada). Primers, antibiotics, the Flp-In^{TM} system, 293/FRT cells, Lipofectamine, PLUS reagent and the pcDNA3 vector were from Invitrogen. Deoxyribonucleic NTPs were obtained from GE Healthcare (Baie d'Urfé, QC, Canada) and the Expand High Fidelity^{PLUS} PCR System polymerase from Roche Applied Sciences (Laval, QC, Canada). RNAqueous®-4PCR system and DNase I were from Ambion (Austin, TX, USA) Restriction endonucleases, modifying enzymes, Standard Taq Polymerase and Phusion DNA polymerase were purchased from New England Biolabs (Ipswich, MA, USA); plasmid DNA purification kits and gel extraction kits were from Qiagen Inc (Mississauga, ON, Canada). pEGFP was obtained from Clontech Laboratories Inc (Mountain View, CA). ACTH (1-24) was purchased from Organon (Toronto, ON, Canada). IBMX (3-isobutyl-1-methylxanthine), cAMP and ATP were from Sigma (Oakville, ON, Canada); [^{3}H]-adenine (25 Ci/mmol) was from Perkin-Elmer (Boston, MA). The mouse monoclonal anti-Myc antibody clone 9E10 was obtained from Dr. Michel Bouvier (Groupe de Recherche Universitaire sur le Médicament, Université de Montréal, Montréal, Québec, Canada) and was used in the form of cleared 9E10 hybridoma culture medium [11]. The anti-6xHis rabbit polyclonal antibody (H15 probe) and the anti-Flag rabbit polyclonal antibody were from Santa Cruz (La Jolla, CA, USA). Mouse monoclonal anti-protein disulfide isomerase (PDI) and anti-giantin were from Abcam (Cambridge, UK). AlexaFluor-coupled secondary antibodies were from Invitrogen. Secondary antibodies coupled to horseradish were from GE Healthcare. All other chemicals were of grade A purity.

Regarding the expression vectors, Myc-MC2R, tagged-MRAP constructions and 6xHis-MRAPdCT-Flag have been described previously [7, 11]. Briefly, MRAPdCT was constructed with the Expand High Fidelity^{PLUS} PCR System. N- and C-terminal epitope-tags were added to MRAPdCT, 6xHis and Flag

respectively. *Spe*I/Kozak/6xHis-MRAP-Flag/*Xba*I cDNA sequences were amplified from the native pcDNA3/MRAPα template. The PCR products were purified, digested and cloned into pcDNA5/FRT, thus yielding MRAPdCT fused at its N- and C-terminus with the 6xHis (MGGSHHHHHH) and Flag (NYDDDDKC) epitopes respectively. ZfMC2R and zfMRAP1 constructions were previously described [10], as well as the MRAP2-Myc construction [11].

2.2. Cell culture, transfection and isogenic cell lines

Native 293/FRT cells (HEK293 cell line with single genome-integrated *Flp* Recombinase Target site (FRT)) were maintained in high-glucose DMEM with 7 % FBS, 2 mM GlutaMAX and 100 µg/ml Zeocin. The *Flp* recombinase-mediated homologous recombination system (Flp-In^{TM} System) was used to generate 293/FRT/gene of interest cell lines stably expressing Myc-MC2R, Myc-zfMC2R, 6xHis-MRAPα-Flag, 6xHis-MRAPβ-Flag and 6xHis-MRAPdCT-Flag and were maintained with 100 µg/ml Hygromycin B according to the manufacturer's recommendations [7]. B16-G4F cells were cultured in high-glucose DMEM with 7 % FBS and 2 mM GlutaMAX. Unless otherwise stated, cells were transfected with 0.5 µg of plasmid DNA per 35 mm dish using Lipofectamine and PLUS reagent. To maintain similar transcriptional and translational activity when required, transfection of pEGFP was used instead of an empty vector as a control.

2.3. Cyclic AMP measurements

Transient transfections were performed 24 h after initial seeding of 4 x 10^5 cells in 35 mm dishes with 0.5 µg of plasmid DNA. Intracellular cAMP accumulation was performed as described previously [7]. Briefly, cells were loaded with tritiated adenine for 2 h, washed once in Hank's buffered saline (130 mM NaCl, 3.5 mM KCl, 1.8 mM $CaCl_2$, 0.5 mM $MgCl_2$, 2.5 mM $NaHCO_2$, 5 mM HEPES, pH 7.4, containing 1 g/l dextrose and 0.1 % BSA) and subsequently stimulated with ACTH, in the presence of the phosphodiesterase inhibitor IBMX (iso-butyl-methyl-xanthine), at 37 °C. At the end of the stimulations, cells were lysed in 5 % trichloroacetic acid (TCA), and intracellular cAMP accumulation was determined by measuring the conversion of [^{3}H]-ATP into [^{3}H]-cAMP eluted from Dowex and neutral alumina chromatography columns.

2.4. Immunofluorescence microscopy

Cells were seeded on poly-L-lysine glass coverslips placed in 35 mm dishes. If required, cells were transfected the following day with 0.5 µg of pcDNA5/FRT/MRAP2-Myc, pcDNA5/FRT/Myc-MC2R, pcDNA5/FRT/Myc-zfMC2R or Rab1-EGFP. The following day, cells were starved for 30 min with fresh DMEM without FBS. After one wash in cold PBS, cells were fixed with MeOH and washed with acetone as previously described [11]. Labeling for Myc-tagged proteins and MRAP-Flag were performed as described previously [7]. Antibodies used for labeling cellular markers or organelles included: mouse anti-PDI (1:2000), mouse anti-Giantin (1:500). Primary antibodies were detected with goat anti-mouse or anti-rabbit secondary antibodies coupled to Alexa-Fluo647 and Alexa-Fluor568 respectively, with DAPI used to stain the nuclei. Images were acquired on an Olympus Fluoview 1000 (FV1000) laser-scanning confocal microscope (Olympus, Japan) using a U Plan S-Apo 60X (1.35 NA) oil immersion objective. Emission from each fluorophore was acquired sequentially to avoid fluorophore bleeding. All images were magnified in Photoshop CS3 (Adobe Systems Inc.). The pixel fluorograms were obtained and analyzed according to the Pearson's correlation coefficient [24] by plotting pixel values of each component relative to the horizontal and vertical axis respectively. Quadrant markers were placed forming background (lower-left), red-only (upper-left), green-only (lower-right) and colocalizing (upper-right) areas. The Pearson's correlation coefficient describes the correlation of the intensity distribution between channels using a scale from 0 to 1, with 0 indicating no significant correlation and 1.0 indicating complete correlation [24].

2.5. Whole cell ELISA procedures

Cell-surface ELISA procedures were carried out as previously described [7]. Briefly, cells were seeded into poly-L-Lysine-coated 24-well plates at 10^5 cells/well and transfected with 0.125 µg DNA/well or as indicated and with pEGFP (subtracted background OD). After 24 h, cells were washed with PBS, fixed on ice for 15 min with 1.85 % formaldehyde, washed, blocked in 10% horse serum and then incubated with a mouse anti-c-Myc mixture (1:666), rabbit anti-Flag (1:200) and/or rabbit anti-6xHis (1:200) antibodies and detected with appropriate secondary antibodies coupled to horseradish peroxidase. Total expression levels were monitored by fixing and permeabilizing cells with 100% MeOH instead of formaldehyde [11]. The

substrate H_2O_2 (0.003%) and the chromophore O-phenylenediamine (1mg/ml) were used to reveal the amount of cell-surface receptors [7]. Total and cell-surface expression levels were normalized to pEGFP transfection levels. In the characterization of MRAP topology, the cell-surface topology assay strictly determines the epitope (Flag or 6xHis) that lies outside unpermeabilized cells and localized at the plasma membrane, and not in other membrane compartments found inside the cells, such as endoplasmic reticulum (ER) membranes. Henceforth, the term cell-surface topology is used to describe these sets of experiments and their interpretations.

2.6. Western blot analyses

For the analyses of MRAP proteins, cells were grown in 35 mm dishes, transfected with 0.5 µg of plasmid at mid-confluency and lysed at confluency in lysis buffer (20 mM Tris-HCl pH 7.5, 150 mM NaCl, 1 mM Na_2EDTA, 1 mM EGTA, 1 % Triton X-100, 2.5 mM Na pyrophosphate, 1 mM β-glycerophosphate, 1 mM Na_3VO_4, 1 µg/ml leupeptin). Samples were processed as described previously [Roy, 2007 #22; Roy, 2010 #21. Proteins transferred onto nitrocellulose membranes were blocked in TBS-Tween 0.05 % (containing 5 % non-fat powdered milk) for at least 30 min, and then incubated with mouse monoclonal anti-c-Myc antibody (1:500), with polyclonal rabbit anti-6xHis (1:1000) or anti-Flag (1:1000) for 1 h. After washing, appropriate secondary antibodies coupled to horseradish peroxidase (HRP) were incubated for 1 h at room temperature and then washed 5 times before detection with enhanced chemiluminescence, according to the manufacturer's instructions. Quantification of blots was normalized to the total level of $p42/p44^{mapk}$, since it was found that the level of actin varies under ACTH stimulation, but not the level of total $p42/p44^{mapk}$. Following incubation with primary antibodies, membranes were stripped for 2 h with glycine 0.2 M (pH 2.5) at 70 °C, then washed, blocked in 1% gelatin, and further incubated with total $p42/p44^{mapk}$ for 16 h (dilution 1:1000). Immunoreactive bands were scanned by laser densitometry and expressed in arbitrary units.

2.7. Immunoprecipitation

Immunoprecipitation was performed as described previously [Parent, 2009 #20]. Briefly, native 293/FRT cells were transiently transfected with empty vector, MRAPα-Flag or MRAPβ-Flag with or

without MRAP2-Myc. After 42 h, cells were collected in lysis buffer and the lysates clarified by centrifugation for 20 min at 14000 *g* at 4 °C. After pellet removal, 2 µg of anti-Flag monoclonal antibodies were added to the supernatants to immunoprecipitate Flag-tagged proteins. After overnight incubation at 4 °C with A-agarose, the immunoprecipitated proteins were washed and eluted by the addition of 50 μl of sample buffer, followed by a 60-min incubation at room temperature (20°C). Initial lysates and immunoprecipitated proteins were resolved by SDS–PAGE on 15 % bis-acrylamide gels and immunoblotting was performed on nitrocellulose membranes using rabbit polyclonal anti-Flag (1:1000) or anti-Myc (1:1000) antibodies.

2.8. Data analysis

The results are presented as mean ± SEM unless stated otherwise. GraphPad Prism 5.0 (GraphPad Software, San Diego, CA) was used to determine the EC_{50}, 95% confidence intervals and maximal effects using log scaled ACTH concentrations (concentration-response curves: log agonist *vs.* response; baseline is shared and fixed between 0 and 0.1 % cAMP/ATP; Hill slopes were fixed at a value of 1.0). EC_{50} values are given with 95% confidence intervals as mean [lower limit, higher limit]. For non-linear regression analyses, p values were obtained with the extra sum-of-squares F test. Statistical analyses for determining significance of other parameters were performed by ANOVA followed by Bonferonni's post-hoc test.

3. Results

3.1 Subcellular localization of human MRAP1 isoforms

Human MRAPα and MRAPβ isoforms do not share more than 3 single amino acids in their spliced C-terminal domains, suggesting isoform- and species-specific functions for this portion of the molecule. Thus, the equivalent of the human N-terminal conserved domain - (MRAP1 amino acids 1-68, called MRAPdCT) - was specifically engineered with an N-terminal 6xHis and a C-terminal Flag-tag in order to delineate the role of the C-terminal domain in MRAP and MC2R functions.

The respective localizations of MRAPα, MRAPβ and MRAPdCT in cells stably expressing these proteins individually (in the absence of MC2R) were investigated by confocal microscopy using C-terminally Flag-tagged MRAPs. MRAPα was preferentially localized in intracellular structures and around the nuclear envelope (Fig. 1A, left panel, a, b, c), while MRAPβ exhibited a strong localization at the plasma membrane, even under basal conditions (Fig. 1B, left panel, a, b, c). Inside the cell, as shown in the merged images and in the fluorograms, MRAPα exhibited a good level of colocalization with protein disulfide isomerase (PDI), a marker of the ER and with the GTPase Rab1 (a marker for the endosomal transport between Golgi and ER), but very weak colocalization with giantin, a cisternae component of the Golgi apparatus (Fig. 1Aa, b, c). In contrast, MRAPβ exhibited only weak or no colocalization with PDI, giantin or Rab1 (Fig. 1Ba, b, c). Finally, the truncated MRAP1, MRAPdCT, was concentrated in regions neighboring the ER, Golgi and in perinuclear regions (Fig. 1Ca, b, c). In B16-G4F cells, only MRAPα and MRAPdCT colocalized with Rab1 (Fig. 2).

The possibility that MRAP1s are also localized in trafficking endosomes was investigated through labeling of endosome markers such as recycling (Rab4), endocytic (Rab5), late (Rab7) and perinuclear endosomes (Rab11) [25, 26]. As shown in the merged images and in fluorograms, a fraction of MRAPα was colocalized with Rab11 and a small fraction with Rab7, but there was no colocalization with Rab 4 or Rab5 (Fig. 3A). On the other hand, a small fraction of MRAPβ was found to colocalize with Rab4, Rab5 and Rab11, but not with Rab7 (Fig. 3B).

3.2. Translocation of MRAP1 isoforms to the plasma membrane by MC2Rs

The ability of MRAP1s to influence MC2R targeting at the plasma membrane was examined by transient transfection of human or zebrafish MC2Rs in stable MRAP1 cell lines. Immunofluorescence experiments revealed that the human MC2R (Myc-hMC2R) in cells stably expressing MRAPα (Fig. 4A) or MRAPβ (Fig. 4B) caused a significant relocalization of MRAPα from its intracellular localization (Fig. 1) to the plasma membrane where it colocalized with MC2R (Fig. 4A, arrows). In these cells the level of expression of MRAPα was increased comparatively to untransfected cells (Fig. 4A upper panel; double-arrow pointing at the upper cell not expressing MC2R). Similar translocation from cytoplasm to plasma membrane was also observed using zebrafish MC2R (Myc-zfMC2R) instead of hMC2R (Fig. 4A, lower panel). Transfection of the cells with human and zfMC2R also induced a complete translocation of MRAPβ from endosomes to the plasma membrane (Fig. 4B). In the case of Myc-zfMC2R however, a large proportion of the receptor remained intracellular (Fig. 4B, lower panel). Interestingly and in contrast with results shown in Fig. 1C, in the presence of human MC2R, MRAPdCT was now expressed at the plasma membrane (Fig. 4C).

Western blotting measurements were performed to validate the immunofluorescence results in which MC2R expression was able to increase MRAP expression. All the bands for MRAPα were discernible in at least five forms (20, 24, 30, 42 and 55 kDa), MRAPβ in at least two forms (18 and 23 kDa) and MRAPdCT in only one form (10 kDa). MRAPα and MRAPdCT expressions were largely increased by MC2R coexpression (– *versus* + lanes) as compared to a loading control (total p44/p42^{mapk}) (Fig. 5A).

Whole cell-based ELISA experiments were also performed to measure cell-surface and total levels of human MC2R in 293/FRT/Myc-MC2R cells (Fig. 5B) and in Myc-zfMC2R (Fig. 5C) transiently expressing the different MRAP1s. As shown in Fig. 5B and C, although the coexpression of different MRAP1s increased both hMC2R cell-surface expression and total expression to various degrees, the increase was higher for cell-surface compared to total expression, and, as previously reported [7, 11], with MRAPβ having a greater effect than MRAPα. MRAPdCT increased MC2R cell-surface expression to

approximately the same extent as that observed with MRAPα while zfMRAP1 was slightly higher than MRAPα.

3.3 Role of MRAP2 in MRAP1 localization

The ability of MRAP2 to influence human MRAP1 isoform localization was examined in transient MRAP2-Myc-transfected cells stably expressing MRAPα-Flag or MRAPβ-Flag. In non-transfected cells, MRAPα was localized as described in Fig. 1 and 3; however, as evidenced in merged images, in MRAP2-transfected cells, MRAPα and MRAP2 colocalized in intracellular compartments (Fig. 6A; arrows in upper panels). In contrast, MRAPβ exhibited only a low level of colocalization with MRAP2 (Fig. 6A, lower panels and fluorogram). A similar tendency for some colocalization between MRAPα-Flag and MRAP2 in intracellular compartments, but not between MRAPβ-Flag and MRAP2, was observed in B16-G4F cells (Fig. 6B).

The interaction between MRAP2-Myc and Flag-tagged MRAP1 isoforms was confirmed by immunoprecipitating the Flag-tagged MRAP1 isoforms. Myc-MRAP2 co-immunoprecipitated with MRAPα-Flag (Fig. 7A, IP lane 4) as described previously [27] and to a lesser extent with MRAPβ-Flag (Fig. 7B, IP lane 4). When compared to a loading control present in cell lysates (total p44/p42^{mapk}) (lower panels in Fig.7B and C), MRAP2 expression was increased by nearly 2-fold when MRAPα or MRAPβ was present (Fig. 7C). Conversely, MRAPα and MRAPβ expressions were also increased by 2-fold when MRAP2 was coexpressed (Fig. 7D).

3.4 Membrane-spanning topology of MRAPα, MRAPβ and MRAPdCT

Measurements of cell-surface expression levels of double-tagged MRAP constructs (6xHis in N-terminus and Flag in C-terminus) were carried out using the non-permeabilized cell-surface ELISA method. MRAPα exhibited a single plasma membrane topology since only the C-terminal Flag tag could be detected outside unpermeabilized cells while double detection with both anti-6xHis and anti-Flag antibodies did not yield any increase in signal detection. In contrast, both N- and the C-terminus of MRAPβ and of MRAPdCT were detected outside the cells and an increase in double detection could be observed with anti-

6xHis and anti-Flag antibodies conjointly, indicating that they were inserted into the plasma membrane in both orientations (Fig. 7C). Nevertheless, the levels of MRAPdCT at the plasma membrane were relatively low as compared to full length MRAP isoforms (N-terminus: MRAPβ > MRAPdCT > MRAPα; C-terminus: MRAPα ≥ MRAPβ > MRAPdCT).

3.5. Influence of MRAP C-terminal domains on MC2R function

To verify the functional impact of different MRAP C-terminal domains on MC2R function, ACTH-induced cAMP production was compared in cells stably expressing human MC2R (293/FRT/Myc-MC2R) and transiently transfected with MRAPα, MRAPβ, MRAPdCT or zfMRAP1. As previously described [6-8, 11, 28], despite the endogenous presence of MRAP2 in 293/FRT cells [10, 11], ACTH does not activate MC2R unless a MRAP1 is present (data not shown). ACTH induced a dose-dependent increase in cAMP with EC_{50} values of 126 [87-182] pM in MRAPα- and of 338 [286-400] pM in MRAPβ-transfected cells (Fig. 8A). With MRAPdCT, cAMP production was obtained at the same threshold concentration of 30 pM ACTH, with an EC_{50} value of 659 [496-873] pM ($p < 0.01$ compared to MRAPβ) and a maximal cAMP accumulation (R_{max}) between that obtained with MRAPα and MRAPβ isoforms [MRAPα (R_{max} = 6.3 ± 0.2 %), MRAPβ (R_{max} = 12.5 ± 0.3 %), MRAPdCT (R_{max} = 9.6 ± 0.4 %), n = 3] ($p < 0.001$ compared to MRAPα and to MRAPβ). With zfMRAP1, cAMP production was obtained at the threshold concentration of 1 pM ACTH with an EC_{50} value of 20 [9-42] pM ($p < 0.001$ compared to MRAPα) and maximal ACTH responses of 7.1 ± 0.2 %. Thus, ACTH potency was as follows: zfMRAP1 > MRAPα > MRAPβ > MRAPdCT and the maximal ACTH responses were MRAPβ > MRAPdCT > zfMRAP1 > MRAPα.

In cells stably expressing the zfMC2R (293/FRT/Myc-zfMC2R) [10], ACTH was unable to stimulate zfMC2R in the absence of zfMRAP1 in 293/FRT cells [10]. However, a linear increase in cAMP accumulation was observed in MRAPα- and MRAPβ-transfected cells since a plateau was not yet reached with 100 nM ACTH (Fig. 8B). Due to incomplete curves with human MRAP1 isoforms, it was not possible to gain further insight on ACTH-induced maximal cAMP responses using zfMC2R and human MRAP1 isoforms. In contrast, in cells expressing zfMRAP1, ACTH stimulation reached a plateau at the concentration of 10 nM, with an EC_{50} of 373 [324, 429] pM, similar to previously published data [10].

These results indicate that zfMRAP1, as compared to MRAPα and MRAPβ, combined to either human or zfMC2R, generated a more sensitive ACTH receptor. From these experiments and from the incomplete curves obtained for cell surface expression, it is tempting to speculate that maximal ACTH responses may reflect cell-surface expression levels (R_{max}: MRAPβ > MRAPα > zfMRAP1).

As shown in Fig.9A, our results confirmed that B16-G4F cells do not express mouse MRAP1 mRNA, therefore MC2R transfection was unable to produce an increase in cAMP upon 100 nM ACTH or 1 μM NDP-MSH (a potent α-MSH analogue, ligand for the MSH receptor, MC1R), in conditions where forskolin (a direct activator of adenylyl cyclases) induced a 40-fold increase over basal level (Fig. 9B). When transiently transfected with MC2R in the presence of MRAPα or MRAPβ, MRAP1 expression enhanced MC2R cell-surface expression in these cells (Fig. 10A). Under these MRAP1-transfected conditions, ACTH increased cAMP accumulation in a dose-dependent manner (Fig. 10B). EC_{50} and R_{max} values obtained with MRAPα (120 [22, 644] pM), MRAPβ (243 [76, 771] pM) and zfMRAP1 (34 [5, 228] pM) were in accordance with the respective results obtained in 293/FRT/Myc-MC2R cells (Fig. 8A), except for the results for MRAPdCT (238 [94, 600] pM) which were similar to the values observed for MRAPβ.

4. Discussion

Using two different cell models which share the lack of MRAP1 and MCR expression, the present study demonstrates that the isoform-specific C-terminal domains of MRAP1s have distinct impacts on the subcellular localization of MRAP1s and on ACTH-induced cAMP signaling. Our results show that MRAPα is preferentially associated with intracellular compartments, while MRAPβ is primarily associated with the plasma membrane. MRAP2 was also found to colocalize with MRAPα and increased its localization at the plasma membrane, as opposed to low or absence of localization with MRAPβ. We also provide evidence that expression of MRAP1 isoforms is increased by both MC2R and MRAP2 coexpression and *vice versa*. Finally, our data clearly indicate that the C-terminal segments of MRAP1 isoforms modulate cAMP responses to ACTH.

Involvement of MRAP1 C-terminal domains in their respective localizations - As shown herein, a large proportion of MRAPα, expressed either alone, with MC2R or with MRAP2, was localized in the endoplasmic reticulum and in Rab1 and Rab11-positive endosomes as well as in vicinity of the nuclear envelope. In contrast, MRAPβ was mainly associated with the plasma membrane, but also partially with recycling endosomes (Rab4 and Rab5). The observation that only a limited fraction of MC2R colocalizes with Rab4 and Rab5 endosomes is in agreement with our recent results that the maximal extent of ACTH-induced MC2R internalization is only from 20 to 30 % and that 28% of the internalized receptors were recycled back to the plasma membrane [26].On the other hand, the truncated MRAP1 version lacking the C-terminal domain (MRAPdCT) was found essentially in the Golgi apparatus and in the early secretory Rab1-positive endosomes, indicating that the C-terminal domains of MRAP1 possess an amino acid motif that is essential for proper sorting from the Golgi apparatus. These findings suggest that in the absence of MC2R, MRAPα is preferentially sorted to pre-Golgi compartments while MRAPβ is preferentially sorted to post-Golgi compartments. Such localizations point to a possible role of MRAPα in the trafficking between the endoplasmic reticulum and Golgi apparatus [25, 29] or may alternatively be involved in an interaction with nucleoporin 50, which has been shown to interact with

MC2R after prolonged ACTH stimulation [30]. In fact, the role of MRAPs in absence of MC2R remains unknown but could likely be differently involved in protein transport unrelated to ACTH signaling, as described initially in adipocytes [31]. Furthermore and importantly, our results show that MRAP1 not only increases MC2R expression, as previously described [8, 11], but that both human and zfMC2R are able to modulate the localization of MRAP isoforms and to promote ACTH signaling, thus indicating that MRAP1 isoform expressions are increased by both MC2R and MRAP2 coexpression.

We found that MRAP2 colocalized massively with MRAPα and increased its localization at the plasma membrane. Accordingly, and as recently observed [27], MRAP2 and MRAPα, as well as MRAP2 and MRAPβ, were found within the same protein complex following immunoprecipitation. These observations are thus is in agreement with other studies indicating that the conserved N-terminal domain is probably sufficient for this interaction [13, 27]. The present results are also in agreement with studies performed in zebrafish, where the coexpression of zfMRAP2a and zfMRAP2b enhanced the effects of zfMRAP1 on zfMC2R signaling [10]. In addition, MRAP1 isoform expression was increased by both MC2R and MRAP2 coexpression, suggesting that MRAP2 may regulate the expression or functionality of various MRAP1s according to the different C-terminal domains of the MRAP1s. However, why or how exactly MRAP2 promotes MRAPα targeting to the plasma membrane remains to be explored in greater detail (for review see [17]), but may be related to physiological events independent from ACTH signaling, such as in protection against cell toxicity [32]. We also found that, at the plasma membrane, MRAPα appeared in the type II (N_{cyto}/C_{exo}) orientation, while MRAPβ and MRAPdCT both exhibited dual-topology (N_{cyto}/C_{exo} and N_{exo}/C_{cyto}). As recently reviewed [13-15], the roles that may be associated with dual-topology of MRAPs proteins remain to be explored and may include interaction with signaling molecules, docking-associated events, molecular chaperoning mechanism, or structural organization, similarly to what is observed during aquaporin-1 topogenesis [33-35].

Role of MRAP1 C-terminal domains on functional MC2R expression - Our data also clearly indicate that the C-terminal segments of MRAP1 isoforms modulate cAMP responses to ACTH. Results herein demonstrate that the truncated MRAPdCT is sufficient to drive functional expression of MC2R. However,

MRAPdCT coexpression with MC2R caused intermediate maximal cAMP responses and lower ACTH potency (decreased sensitivity for cAMP production) indicating that the C-termini of human MRAP1 isoforms are involved in signaling events by increasing ACTH potency for MC2R. This may occur by modifying the affinity of MC2R for ACTH [7]. In turn, ACTH potency may be MRAP1 isoform-dependent and species-specific since the C-terminal domains of zfMRAP1, mouse and human MRAP1s are drastically different. Indeed, zfMRAP1 protein has a major enhancing effect on ACTH potency. On the other hand, maximal responses obtained using the different MRAP1s are correlated with the cell surface expression of MC2R. Thus, the C-terminal domain confers differential capacity (maximal response) and sensitivity to the receptor. In addition, because the C-teminal domain of the zfMRAP1 is completely different in terms of sequence from human MRAP1 isoforms, the results of the zMRAP1 experiments performed herein fully support and corroborate data obtained with the human MRAP1 isoforms.

In summary, our results indicate that MRAPα as well as MRAPdCT are preferentially localized within intracellular compartments associated with early events of the secretory pathway (Rab1, Rab11). In contrast, MRAPβ is mainly associated with plasma membrane and recycling endosomes (Rab4 and Rab5). These findings suggest that the C-terminal domain of MRAPα is responsible for MC2R targeting to the plasma membrane while MRAPβ, with its distinctive C-terminal topology, enhances ACTH-MC2R coupling to adenylyl cyclase activation and cAMP accumulation, potentially aiding in the rapid internalization and recycling of MC2R to the plasma membrane, as recently demonstrated by our group [26].

References

[1] N. Gallo-Payet, M. D. Payet, Mechanism of action of ACTH: beyond cAMP, Microsc Res Tech 61 (2003) 275-287.

[2] M. B. Sewer, M. R. Waterman, ACTH modulation of transcription factors responsible for steroid hydroxylase gene expression in the adrenal cortex, Microsc Res Tech 61 (2003) 300-307.

[3] Y. Xing, C. R. Parker, M. Edwards, W. E. Rainey, ACTH is a potent regulator of gene expression in human adrenal cells, J Mol Endocrinol 45 (2010) 59-68.

[4] K. G. Mountjoy, L. S. Robbins, M. T. Mortrud, R. D. Cone, The cloning of a family of genes that encode the melanocortin receptors, Science 257 (1992) 1248-1251.

[5] R. J. Lefkowitz, J. Roth, W. Pricer, I. Pastan, ACTH receptors in the adrenal: specific binding of ACTH-125I and its relation to adenyl cyclase, Proc Natl Acad Sci U S A 65 (1970) 745-752.

[6] L. A. Metherell, J. P. Chapple, S. Cooray, A. David, C. Becker, F. Ruschendorf, D. Naville, M. Begeot, B. Khoo, P. Nurnberg, A. Huebner, M. E. Cheetham, A. J. Clark, Mutations in MRAP, encoding a new interacting partner of the ACTH receptor, cause familial glucocorticoid deficiency type 2, Nat Genet 37 (2005) 166-170.

[7] S. Roy, M. Rached, N. Gallo-Payet, Differential regulation of the human adrenocorticotropin receptor [melanocortin-2 receptor (MC2R)] by human MC2R accessory protein isoforms alpha and beta in isogenic human embryonic kidney 293 cells, Mol Endocrinol 21 (2007) 1656-1669.

[8] J. A. Sebag, P. M. Hinkle, Melanocortin-2 receptor accessory protein MRAP forms antiparallel homodimers, Proc Natl Acad Sci U S A 104 (2007) 20244-20249.

[9] J. A. Sebag, P. M. Hinkle, Regions of Melanocortin 2 (MC2) Receptor Accessory Protein Necessary for Dual Topology and MC2 Receptor Trafficking and Signaling, J Biol Chem 284 (2009) 610-618.

[10] M. J. Agulleiro, S. Roy, E. Sanchez, S. Puchol, N. Gallo-Payet, J. M. Cerda-Reverter, Role of melanocortin receptor accessory proteins in the function of zebrafish melanocortin receptor type 2, Mol Cell Endocrinol 320 (2010) 145-152.

[11] S. Roy, B. Perron, N. Gallo-Payet, Role of asparagine-linked glycosylation in cell surface expression and function of the human adrenocorticotropin receptor (melanocortin 2 receptor) in 293/FRT cells, Endocrinology 151 (2010) 660-670.

[12] J. A. Sebag, P. M. Hinkle, Regulation of G protein-coupled receptor signaling: specific dominant-negative effects of melanocortin 2 receptor accessory protein 2, Sci Signal 3 (2010) ra28.

[13] P. M. Hinkle, J. A. Sebag, Structure and function of the melanocortin2 receptor accessory protein (MRAP), Mol Cell Endocrinol 300 (2009) 25-31.

[14] T. R. Webb, A. J. Clark, Minireview: the melanocortin 2 receptor accessory proteins, Mol Endocrinol 24 (2010) 475-484.

[15] S. N. Cooray, A. J. Clark, Melanocortin receptors and their accessory proteins, Mol Cell Endocrinol 331 (2010) 215-221.

[16] A. Xu, K. L. Choi, Y. Wang, P. A. Permana, L. Y. Xu, C. Bogardus, G. J. Cooper, Identification of novel putative membrane proteins selectively expressed during adipose conversion of 3T3-L1 cells, Biochem Biophys Res Commun 293 (2002) 1161-1167.

[17] L. F. Chan, L. A. Metherell, A. J. Clark, Effects of melanocortins on adrenal gland physiology, Eur J Pharmacol 660 (2011) 171-180.

[18] S. N. Cooray, A. J. Clark, Melanocortin receptors and their accessory proteins, Mol Cell Endocrinol 331 (2011) 215-221.

[19] J. M. Cerda-Reverter, M. J. Agulleiro, R. G. R, E. Sanchez, R. Ceinos, J. Rotllant, Fish melanocortin system, Eur J Pharmacol 660 (2011) 53-60.

[20] L. Liang, J. A. Sebag, L. Eagelston, M. N. Serasinghe, K. Veo, C. Reinick, J. Angleson, P. M. Hinkle, R. M. Dores, Functional expression of frog and rainbow trout melanocortin 2 receptors using heterologous MRAP1s, Gen Comp Endocrinol 174 (2011) 5-14.

[21] N. Gallo-Payet, E. Escher, Adrenocorticotropin receptors in rat adrenal glomerulosa cells, Endocrinology 117 (1985) 38-46.

[22] N. Gallo-Payet, E. Grazzini, M. Côté, L. Bilodeau, A. Chorvatova, M. D. Payet, L. Chouinard, G. Guillon, Role of calcium in the mechanism of action of ACTH in human adrenocortical cells., J. Clin. Invest. 98 (1996) 460-466.

[23] F. F. Solca, J. Chluba-de Tapia, K. Iwata, A. N. Eberle, B16-G4F mouse melanoma cells: an MSH receptor-deficient cell clone, FEBS Lett 322 (1993) 177-180.

[24] V. Zinchuk, O. Zinchuk, T. Okada, Quantitative colocalization analysis of multicolor confocal immunofluorescence microscopy images: pushing pixels to explore biological phenomena, Acta Histochem Cytochem 40 (2007) 101-111.

[25] F. Jean-Alphonse, A. C. Hanyaloglu, Regulation of GPCR signal networks via membrane trafficking, Mol Cell Endocrinol 331 (2011) 205-214.

[26] S. Roy, S. J. Roy, S. Pinard, L. D. Taillefer, M. Rached, J. L. Parent, N. Gallo-Payet, Mechanisms of Melanocortin-2 Receptor (MC2R) Internalization and Recycling in Human Embryonic Kidney (HEK) Cells: Identification of Key Ser/Thr (S/T) Amino Acids, Mol Endocrinol (2011).

[27] L. F. Chan, T. R. Webb, T. T. Chung, E. Meimaridou, S. N. Cooray, L. Guasti, J. P. Chapple, M. Egertova, M. R. Elphick, M. E. Cheetham, L. A. Metherell, A. J. Clark, MRAP and MRAP2 are bidirectional regulators of the melanocortin receptor family, Proc Natl Acad Sci U S A 106 (2009) 6146-6151.

[28] S. Roy, S. Pinard, L. Chouinard, N. Gallo-Payet, Adrenocorticotropin (ACTH) effects on MAPK phosphorylation in human fasciculata cells and in embryonic kidney 293 cells expressing human

melanocortin 2 receptor (MC2R) and MC2R accessory protein (MRAP)beta., Mol Cell Endocrinol 336 (2011) 31-40.

[29] L. Achour, C. Labbe-Jullie, M. G. Scott, S. Marullo, An escort for GPCRs: implications for regulation of receptor density at the cell surface, Trends Pharmacol Sci 29 (2008) 528-535.

[30] M. Doufexis, H. L. Storr, P. J. King, A. J. Clark, Interaction of the melanocortin 2 receptor with nucleoporin 50: evidence for a novel pathway between a G-protein-coupled receptor and the nucleus, FASEB J 21 (2007) 4095-40100.

[31] B. A. Boston, The role of melanocortins in adipocyte function, Ann N Y Acad Sci 885 (1999) 75-84.

[32] G. W. Hwang, S. E. Oh, T. Takahashi, J. Y. Lee, A. Naganuma, siRNA-mediated knockdown of the melanocortin 2 receptor accessory protein 2 (MRAP2) gene confers resistance to methylmercury on HEK293 cells, J Toxicol Sci 35 (2010) 947-950.

[33] W. R. Skach, V. R. Lingappa, Transmembrane orientation and topogenesis of the third and fourth membrane-spanning regions of human P-glycoprotein (MDR1), Cancer Res 54 (1994) 3202-3209.

[34] T. M. Buck, W. R. Skach, Differential stability of biogenesis intermediates reveals a common pathway for aquaporin-1 topological maturation, J Biol Chem 280 (2005) 261-269.

[35] Y. Dohke, R. J. Turner, Evidence that the transmembrane biogenesis of aquaporin 1 is cotranslational in intact mammalian cells, J Biol Chem 277 (2002) 15215-15219.

Acknowledgements / Footnotes

*We thank Lucie Chouinard for her experimental assistance. We thank Dr Alex Eberle (Department of Biomedicine, University Hospital Basel, Switzerland) for providing us with the B16-G4F cell line, and Dr. Michel Bouvier (Canada Research Chair in Signal Transduction and Molecular Pharmacology, Groupe de Recherche Universitaire sur le Médicament, Université de Montréal, Montréal, Québec, Canada) for providing the anti-Myc antibody. We thank Drs. Robert Dumaine and Philippe Sarret for use of their confocal microscope and Jean Lainé for help with confocal studies. We are also grateful to Pierre Pothier for critical review of the manuscript.

**This work was supported by grants from the Canadian Institutes of Health Research to N.G.-P. (MOP-82819) and to J.L.P. (MOP-69085) and by the Canada Research Chairs Program. N.G.-P. is a recipient of a Canada Research Chair in Endocrinology of the Adrenal Gland; J.L.P. is a recipient of a Chercheur-boursier senior scholarship from the Fonds de la Recherche en Santé du Québec. N.G.-P. and J.-L.P. are members of the FRSQ-funded Centre de Recherche Clinique Étienne-le Bel. J.M.C-R is a recipient of research funds from the Spanish Science and Innovation Ministry (AGL2010-22247-C03-01, CSD 2007-00002). S.R. is a recipient of a studentship from the Fonds de la Recherche en Santé du Québec. MJA is a recipient of a "Juan de la Cierva" research contract (2009) from the Spanish Science and Innovation Ministry.

***Conflict of interest: S.R., S.J.R., S.P., M..J.A, J.M.C.-R., J.-L.P. and N.G.-P have nothing to declare.

Figure legends

Fig. 1. Influence of the C-terminal domain of MRAPα and of MRAPβ on their localization in HEK293 cells. Confocal microscopy images of cells stably expressing 6xHis-MRAP-Flag in the absence of human MC2R. Cells were labeled for MRAPα (A), MRAPβ (B) or MRAPdCT (C) (all Flag-tagged and with specific antibodies against either protein disulfide isomerase (PDI) as a marker of the endoplasmic reticulum (ER) (a), giantin, as a marker of Golgi cisternae (b) or labeled by Rab1-EGFP for ER-to-Golgi endosomes (c). Colocalization fluorograms based on 3D reconstructions are shown in the right column. The x axis of the fluorograms is representative of green labeling and the y axis is representative of red staining. Colocalization between green-labeling and red-labeling voxels is shown as being proportional to each other in the fluorograms and corresponds to the yellow color in merged slices. Images are representative of three independent experiments where at least 50 cells were examined. Scale bars: 10 µm. Arrows point to colocalization (yellow pseudo-color).

Fig. 2. Influence of the C-terminal domain of MRAP1s for their localization with Rab1 in B16-G4F cells. Confocal microscopy images of B16-G4F cells transiently expressing 6xHis-MRAPα-Flag, 6xHis-MRAPβ-Flag or 6xHis-MRAPdCT-Flag and Rab1-EGFP in the absence of MC2R. Fixed cells were labeled for MRAP1s (Flag tag; red) and Rab1-EGFP (green). Images are representative of two independent experiments where at least 30 cells were examined. Scale bars: 10 µm.

Fig. 3. Influence of the C-terminal domain of human MRAP1 isoforms on their trafficking in endosomes. Confocal microscopy images of cells stably expressing 6xHis-MRAPα-Flag (A) or 6xHis-MRAPβ-Flag (B) in the absence of human MC2R. Cells were labeled for MRAP1s (Flag-tagged and by transient transfection of Rab4-, Rab5-, Rab7- or Rab11-EGFP). Images are representative of two independent experiments where at least 50 cells were examined. Scale bar: 10 µm (equivalent for all images). Arrows

point to colocalization (yellow pseudo-color). Colocalization fluorograms based on 3D reconstructions are shown in the right column, as described in Fig. 3.

Fig. 4. Influence of MC2R expression on human MRAP1 localizations and expressions. Confocal microscopy images of cells stably expressing 6xHis-MRAPα-Flag (A), 6xHis-MRAPβ-Flag (B) or 6xHis-MRAPdCT-Flag (C) in the presence of transiently transfected human Myc-MC2R (Myc-hMC2R) or zebrafish Myc-MC2R (Myc-zfMC2R) (upper and lower images respectively). Fixed cells were labeled for MRAP (Flag-tagged and Myc-tagged receptors. Arrows point at the colocalization between red (MRAP) and green (MC2Rs) channels which yield a yellow color in merged images. In one exception, a horizontal double arrow points to a cell not expressing human Myc-MC2R in panel A. Images are representative of two independent experiments where at least 50 cells were examined. Scale bar: 10 µm.

Fig. 5. Influence of MRAP1 on MC2R expression. A) Immunoblots of proteins collected from native 293/FRT cells transiently expressing 6xHis-MRAPα-Flag, 6xHis-MRAPβ-Flag or 6xHis-MRAPdCT-Flag with (+) or without (-) MC2R and probed for the Flag-tag (upper panel) or stripped and probed for the unphosphorylated forms of p44/p42 (lower panel). *M* (molecular mass in kDa) is shown on the right. The blots are representative of three independent experiments; nsp, non specific band. B, C) 293/FRT/Myc-MC2R cells (human MC2R) (B) and 293/FRT/zfMC2R cells (C) were transfected with pEGFP (subtracted background OD) and transiently transfected with full-length MRAP1s or the truncated MRAPdCT. Cell-surface and total Myc-MC2R expression was measured by ELISA as described in Methods. Results represent the mean ± SEM of three experiments, each performed in triplicate. *, $p < 0.05$; **, $p < 0.01$ and ***, $p < 0.001$, compared with control or indicated conditions.

Fig. 6. Influence of MRAP2 on human MRAP1 isoform localization in 293/FRT/Myc-MC2R cells (human MC2R) (A) and B16-G4F cells (B). Confocal microscopy images acquired from cells stably expressing 6xHis-MRAPα-Flag (upper images) or 6xHis-MRAPβ-Flag (lower images) transiently expressing

MRAP2-Myc. Fixed cells were labeled for MRAP1s (Flag-tagged) and for MRAP2-Myc (Myc-tagged). Images are representative of three independent experiments where at least 50 cells were examined. Scale bar: 10 µm. Arrows point to colocalization (yellow pseudo-color).

Fig. 7. Western blotting before (lysates) and after immunoprecipitation (IP) of 6xHis-MRAPα-Flag (A) or 6xHis-MRAPβ-Flag (B) transiently expressed or not with MRAP2-Myc in 293/FRT cells. For Western blotting, membranes were incubated with anti-c-Myc antibody, then stripped, washed and further incubated with anti-Flag antibody and then with total p42/p44^{mapk} (p44/p42) for quantification, as described in Materials and Methods. Molecular mass (M) in kDa is shown on the left. C) Quantification of MRAP2 and p44/p42^{mapk} expression in cell lysates with and without MRAP1 isoform expression. D) Quantification of MRAPα, MRAPβ and p44/p42^{mapk} expression in cell lysates with and without MRAP2 expression. Results represent the mean ± SEM of three experiments, each performed in triplicate. E) Membrane-spanning topology of human MRAP1 isoforms. Cell-surface ELISA performed on fixed and unpermeabilized 293/FRT cells transiently expressing a GFP (CTL), 6xHis-MRAPα-Flag, 6xHis-MRAPβ-Flag or 6xHis-MRAPdCT-Flag. In different sets of wells, epitope tags exposed outside the cells were detected with rabbit anti-Flag or anti-6xHis antibodies or with both antibodies to allow the detection of either N-terminal or C-terminal tags or both simultaneously. Primary antibodies were detected with the same secondary antibodies linked to HRP. Statistical significance: *: $p < 0.05$, **: $p < 0.01$ and *** $p < 0.001$. Results represent the mean ± SEM of four experiments, each performed in triplicate.

Fig. 8. Influence of MRAP1 C-terminal domains on ACTH-induced cAMP accumulation**.** 293/FRT/Myc-MC2R cells (human MC2R, hMC2R) (A) or 293/FRT/Myc-zfMC2R cells (zebrafish MC2R, zfMC2R) (B) transiently expressing full-length MRAP1s or the truncated MRAPdCT were incubated with increasing ACTH concentrations in order to measure cAMP accumulation, as described in Methods. Results represent the mean ± SEM of three experiments, each performed in triplicate.

Fig. 9. B16-G4F cells do not express mouse MRAP1 and transfected MC2R is non-functional in these cells. A) Reversed-transcribed total RNA from M3 and B16-G4F cells was subjected to PCR against mouse MRAP1 (125 bp). B) B16-G4F cells transfected with an empty vector (pcDNA3) or with Myc-MC2R (pcDNA3/Myc-MC2R) were challenged for 15 min with vehicle, 100 nM ACTH, 1 µM NDP-MSH (a potent α-MSH analogue, ligand for the MSH receptor, MC1R) or 1 µM FSK (forskolin) (a direct activator of adenylyl cyclases) in the presence of 1 mM IBMX (phosphodiesterase inhibitor). Results are the mean ± SE of two independent experiments.

Fig. 10. Localization of MC2R and MRAP1 isoforms in B16-G4F cells (A) and influence of MRAP1 C-terminal domains on MC2R function in B16-G4F cells (B). A) Confocal microscopy images acquired from cells transiently expressing Myc-MC2R alone (left images) or coexpressing MRAPα-Flag (middle images) or MRAPβ-Flag (right images). Fixed and permeabilized cells were labeled for MRAP1s (Flag tag; red pseudocolor) and for Myc-MC2R (Myc tag; green pseudocolor) and counterstained with DAPI (nuclei; blue pseudocolor). Images are representative of two independent experiments where at least 50 cells were examined. Arrow indicates membrane localization of MC2R. Scale bar: 10 µm. B) ACTH-induced concentration-response curves performed on B16-G4F cells transiently expressing human MC2R and MRAPα, MRAPβ, MRAPdCT or zfMRAP1. The inset shows the normalized curves from 0 to 100% of each curve in order to better illustrate the changes in EC_{50} values (n = 3). B: basal.

Figure 1

Figure 1

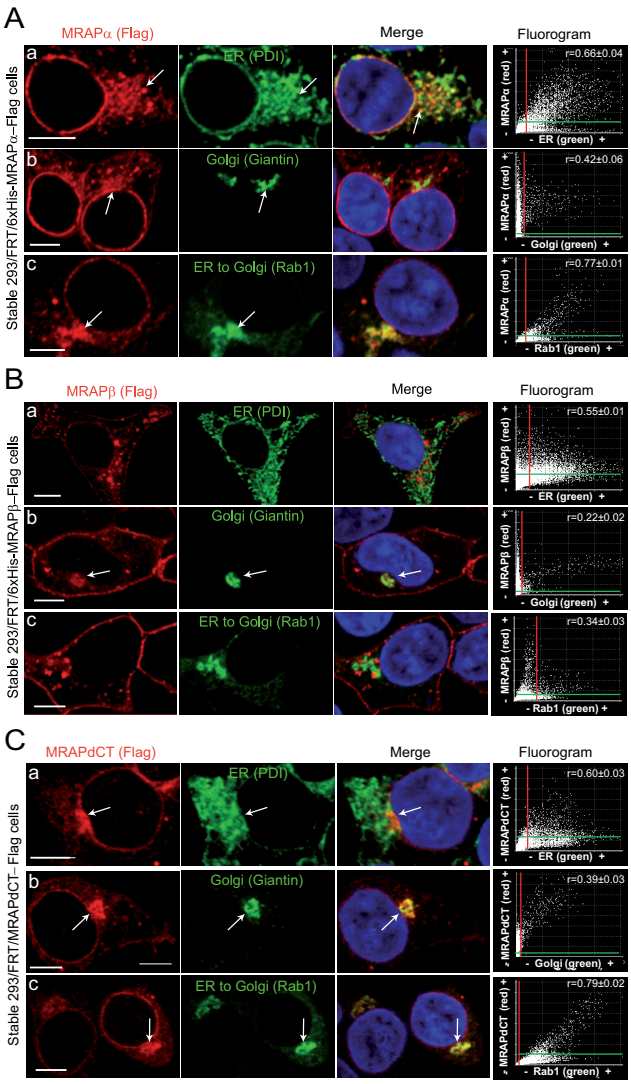

Roy S et al., 2011

Figure 2

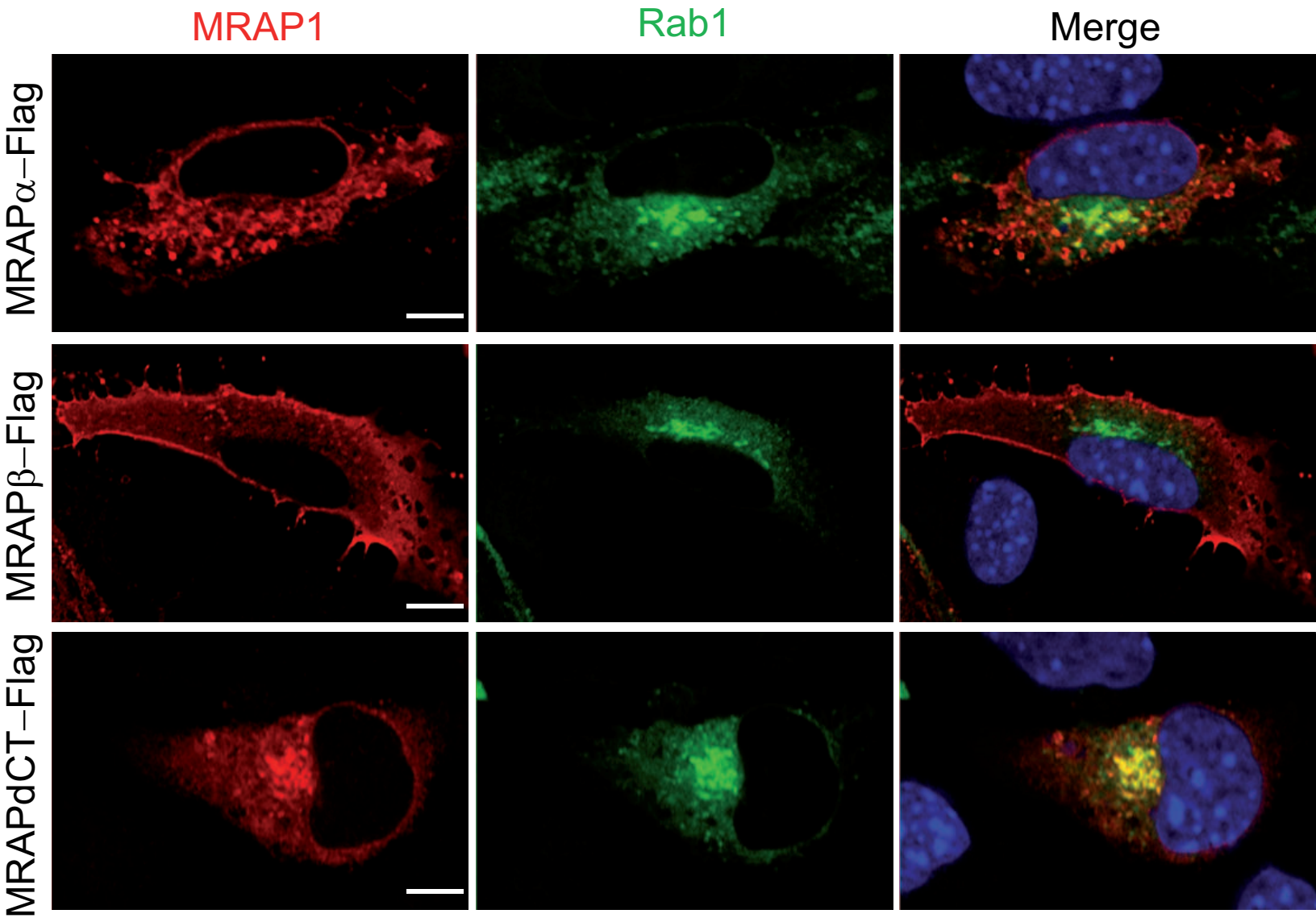

Figure 3

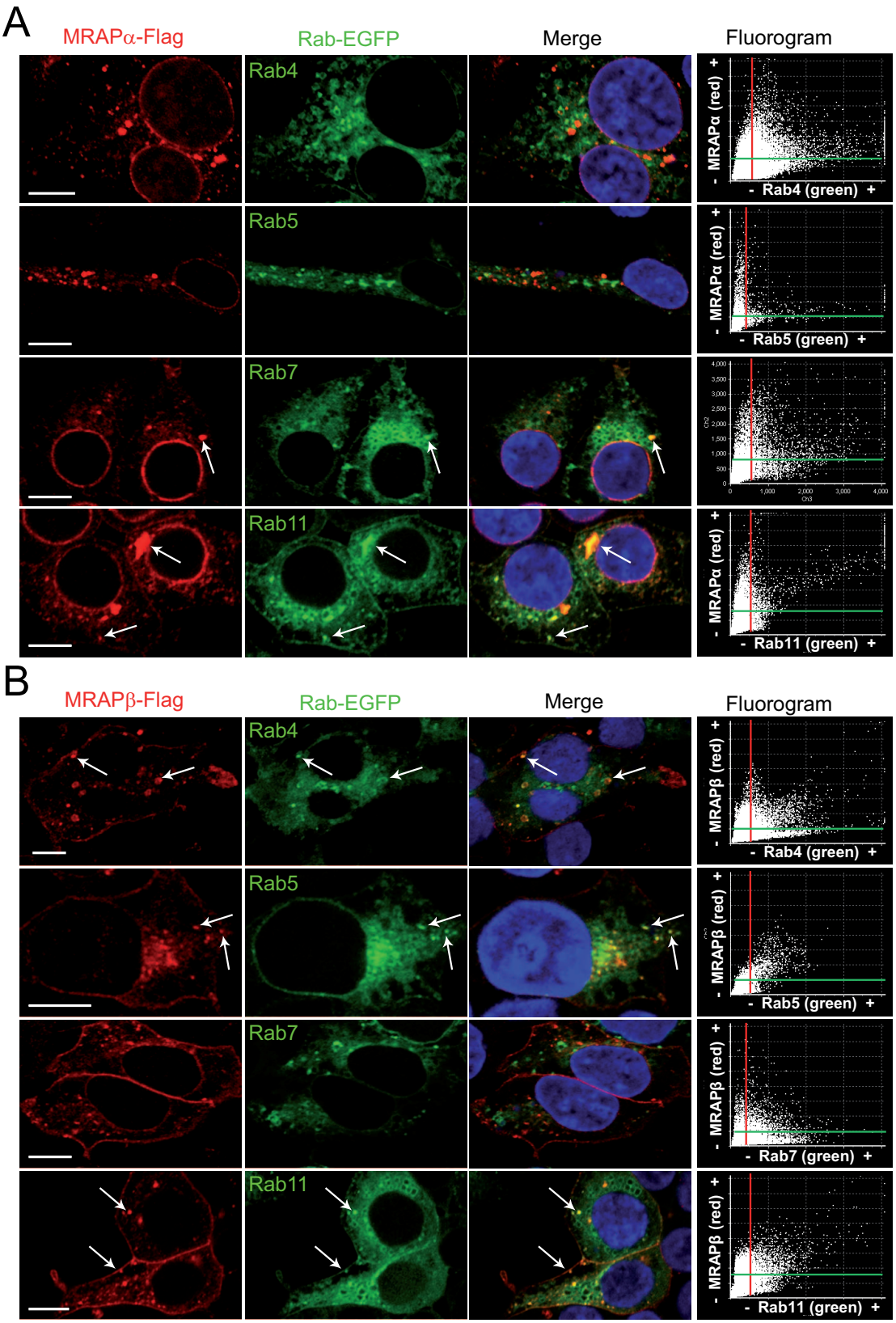

Roy S et al., 2011

Figure 4

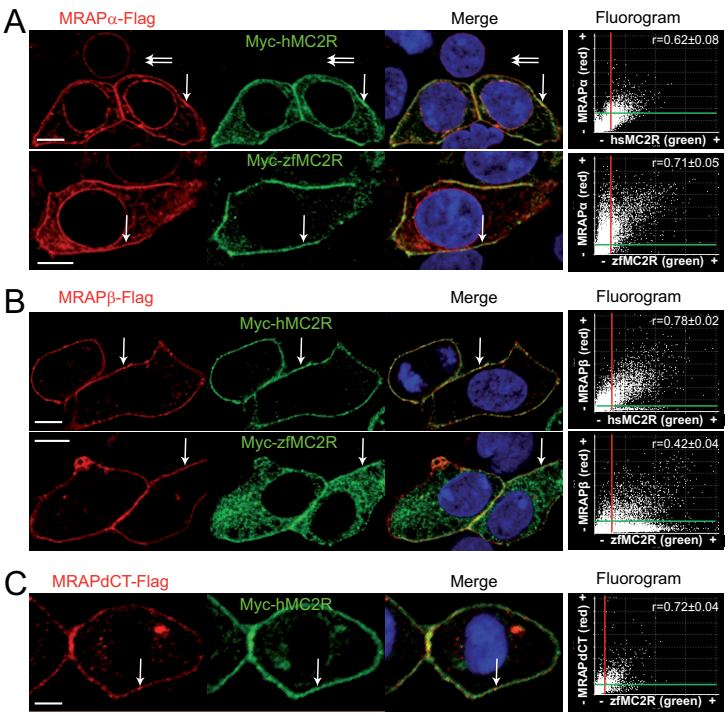
Figure 4
A
MRAPα-Flag
Myc-hMC2R
Merge
Fluorogram
r=0.62±0.08
- MRAPα (red) +
- hsMC2R (green) +
Myc-zfMC2R
r=0.71±0.05
- MRAPα (red) +
- zfMC2R (green) +
B
MRAPβ-Flag
Myc-hMC2R
Merge
Fluorogram
r=0.78±0.02
- MRAPβ (red) +
- hsMC2R (green) +
Myc-zfMC2R
r=0.42±0.04
- MRAPβ (red) +
- zfMC2R (green) +
C
MRAPdCT-Flag
Myc-hMC2R
Merge
Fluorogram
r=0.72±0.04
- MRAPdCT (red) +
- zfMC2R (green) +

Figure 5

Figure 5

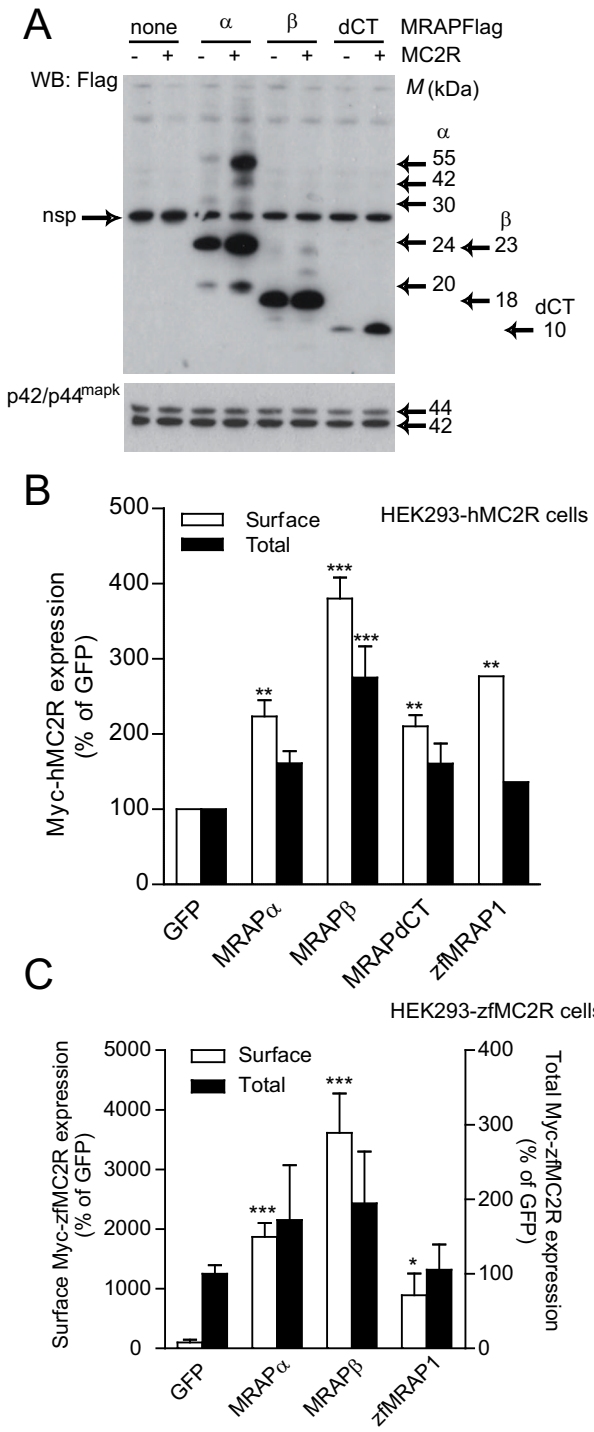

Roy S et al., 2011

Figure 6

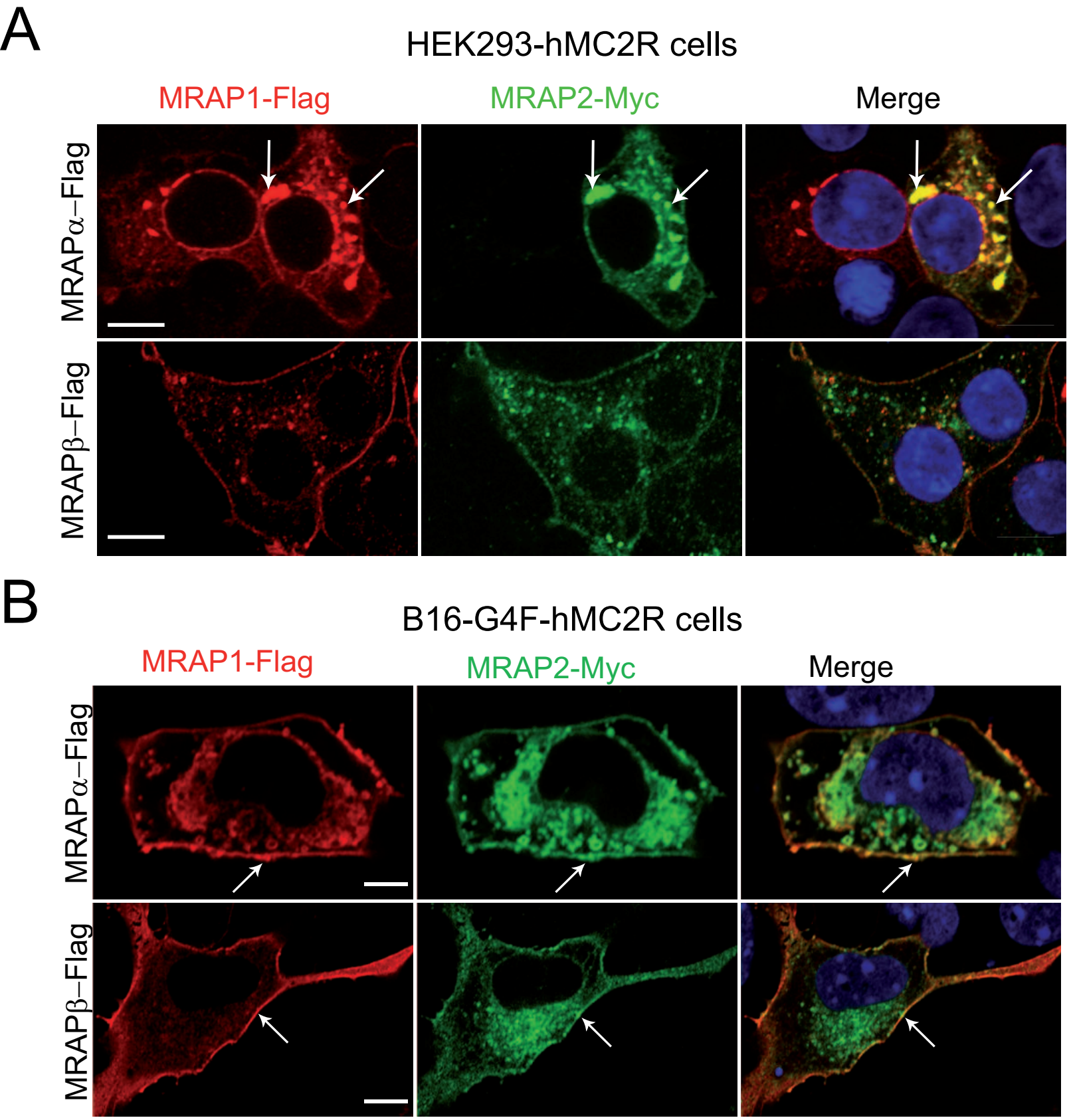

Roy S et al., 2011

Figure 7

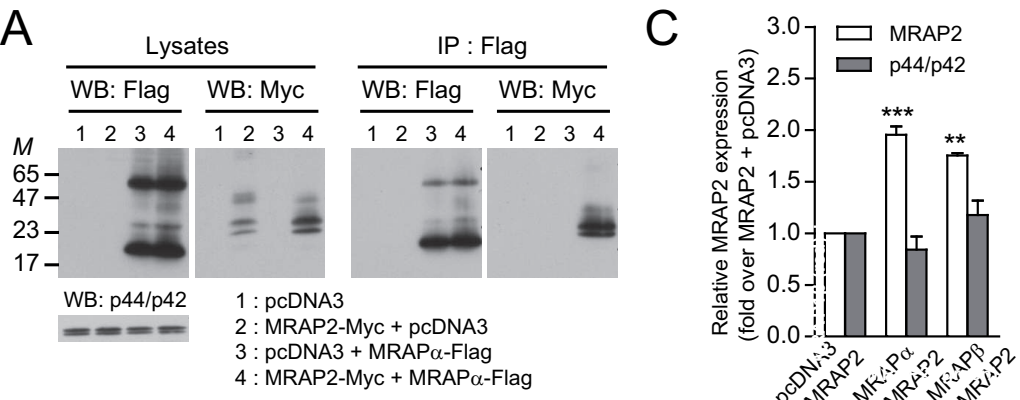

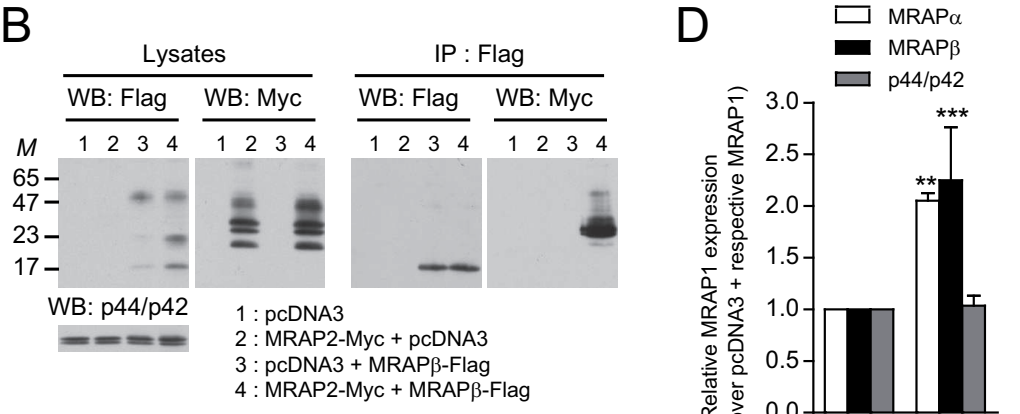

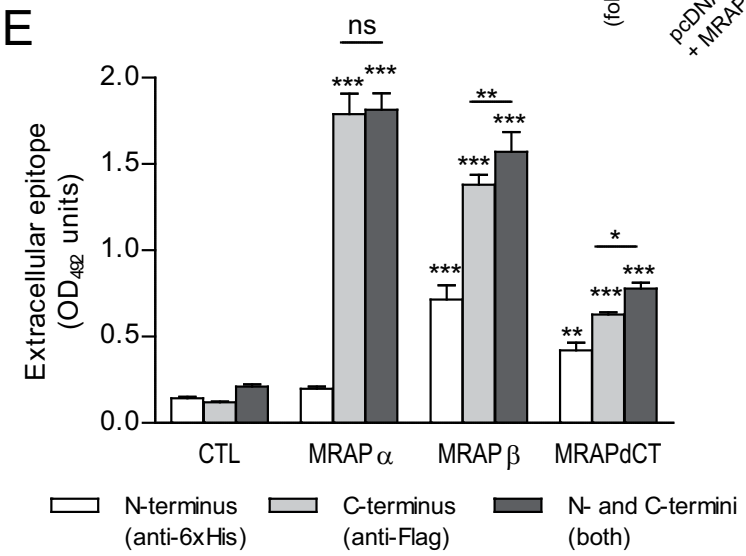

Roy S et al., 2011

Figure 8

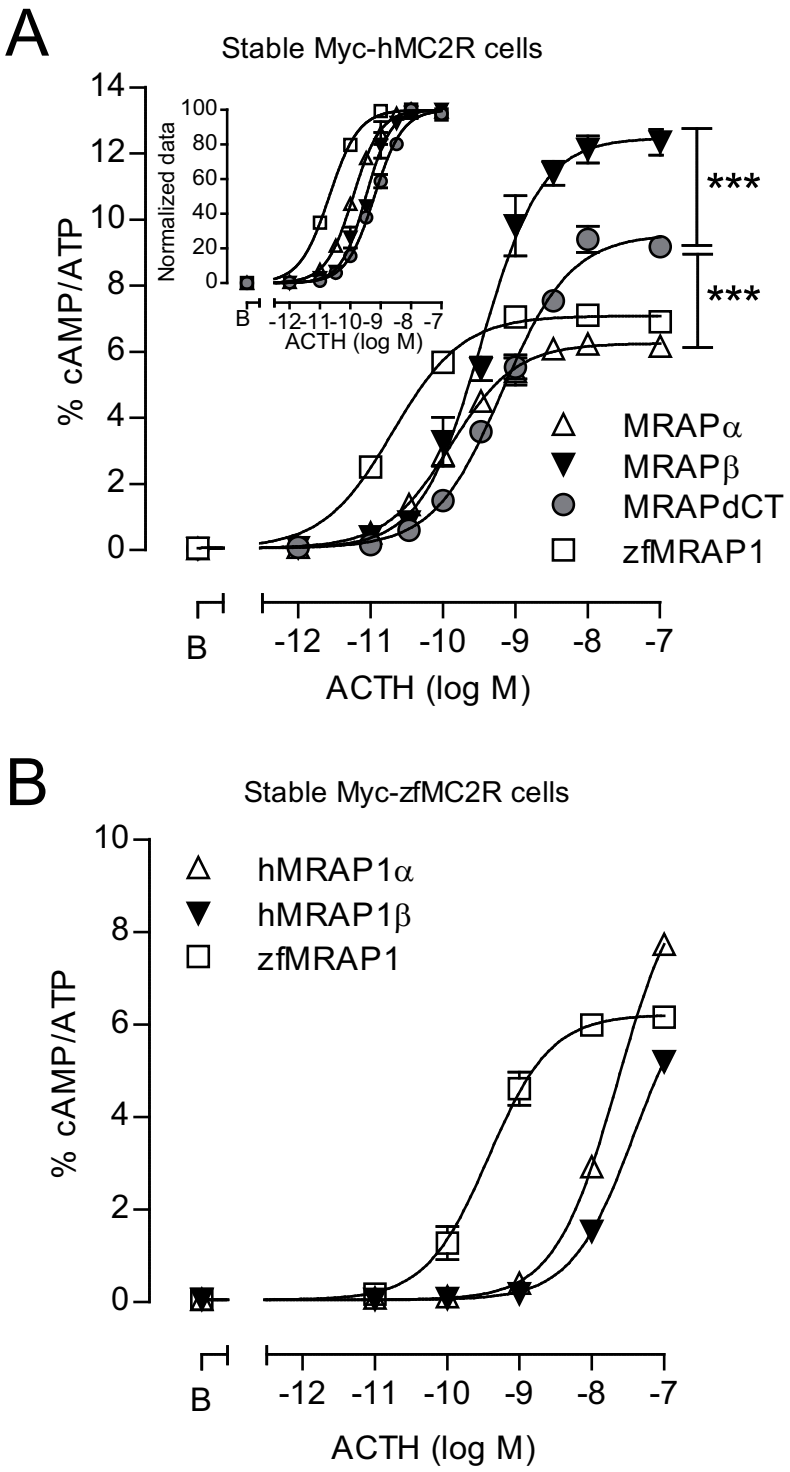
A
Stable Myc-hMC2R cells
% cAMP/ATP
Normalized data
ACTH (log M)
***
***
MRAPα
MRAPβ
MRAPdCT
zfMRAP1
B
-12 -11 -10 -9 -8 -7
ACTH (log M)
B
Stable Myc-zfMC2R cells
% cAMP/ATP
hMRAP1α
hMRAP1β
zfMRAP1
B
-12 -11 -10 -9 -8 -7
ACTH (log M)

Figure 9

Figure 9

A

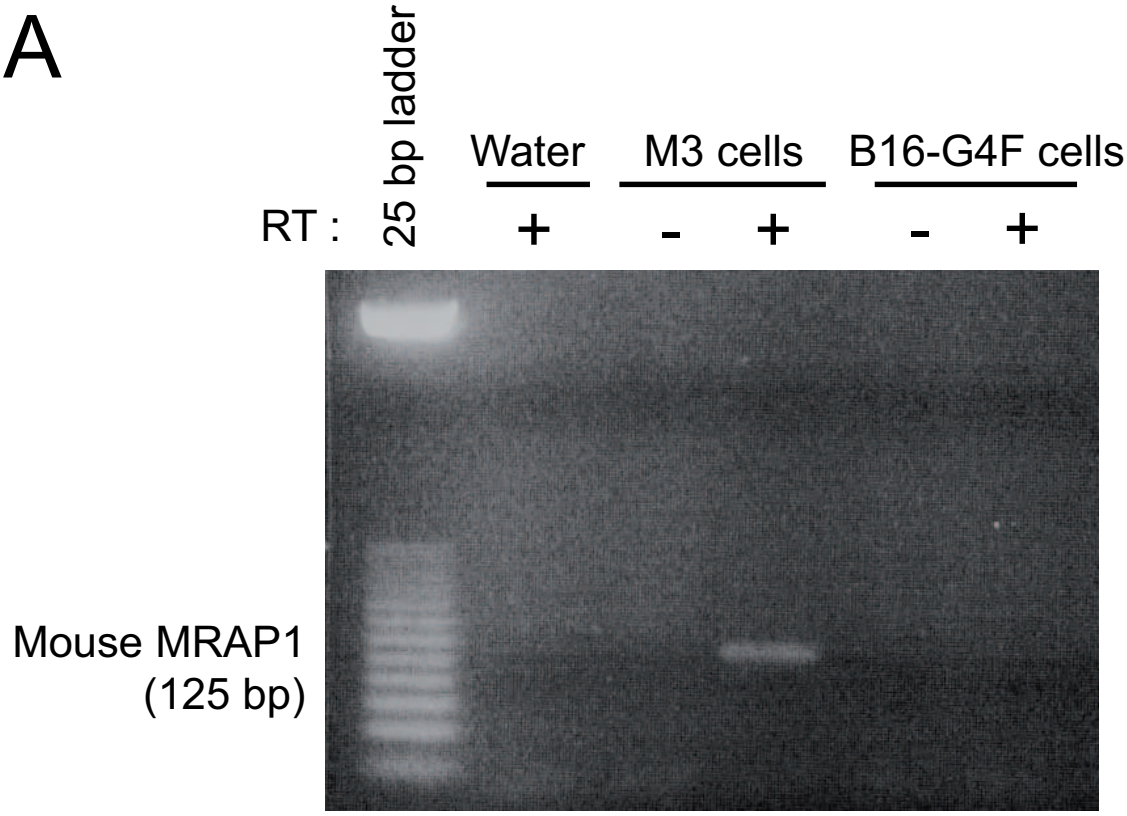

B

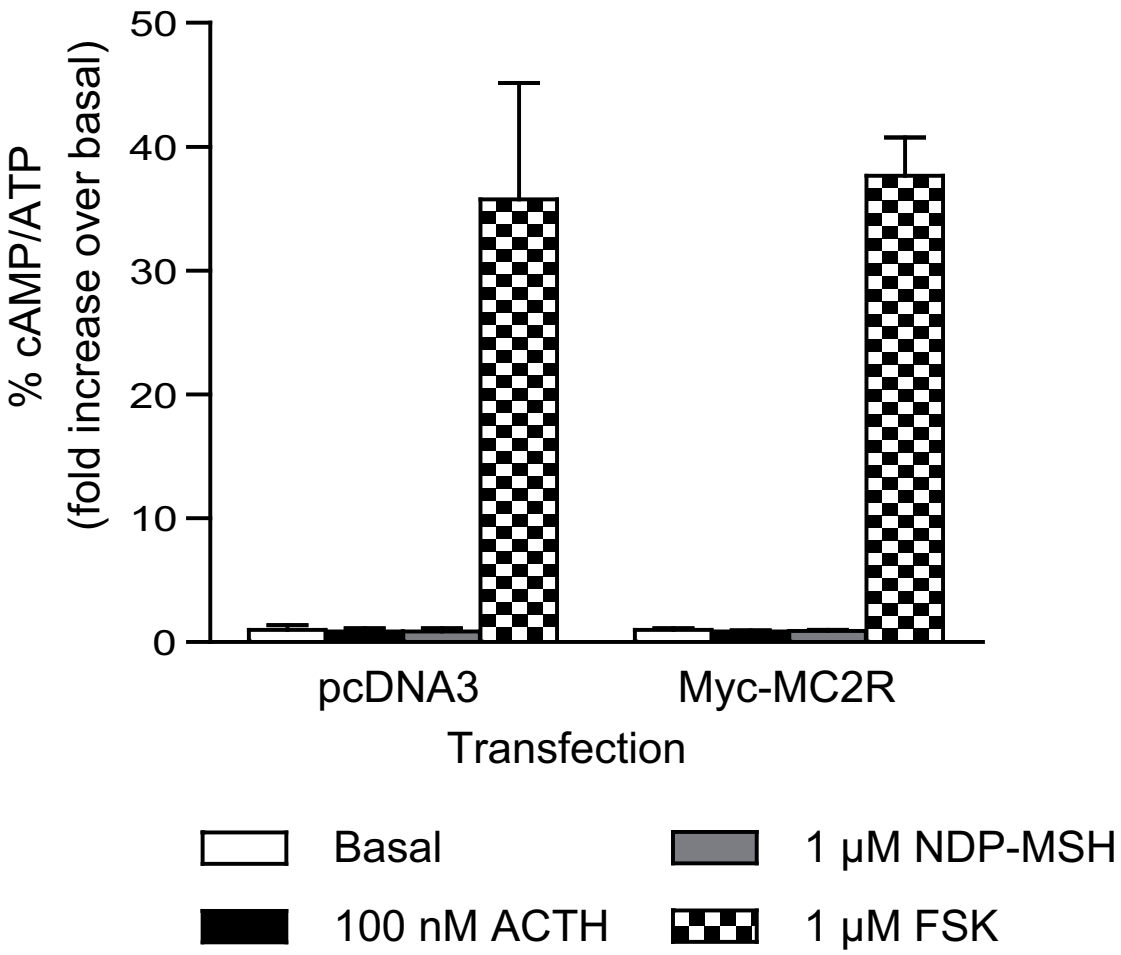

Figure 10

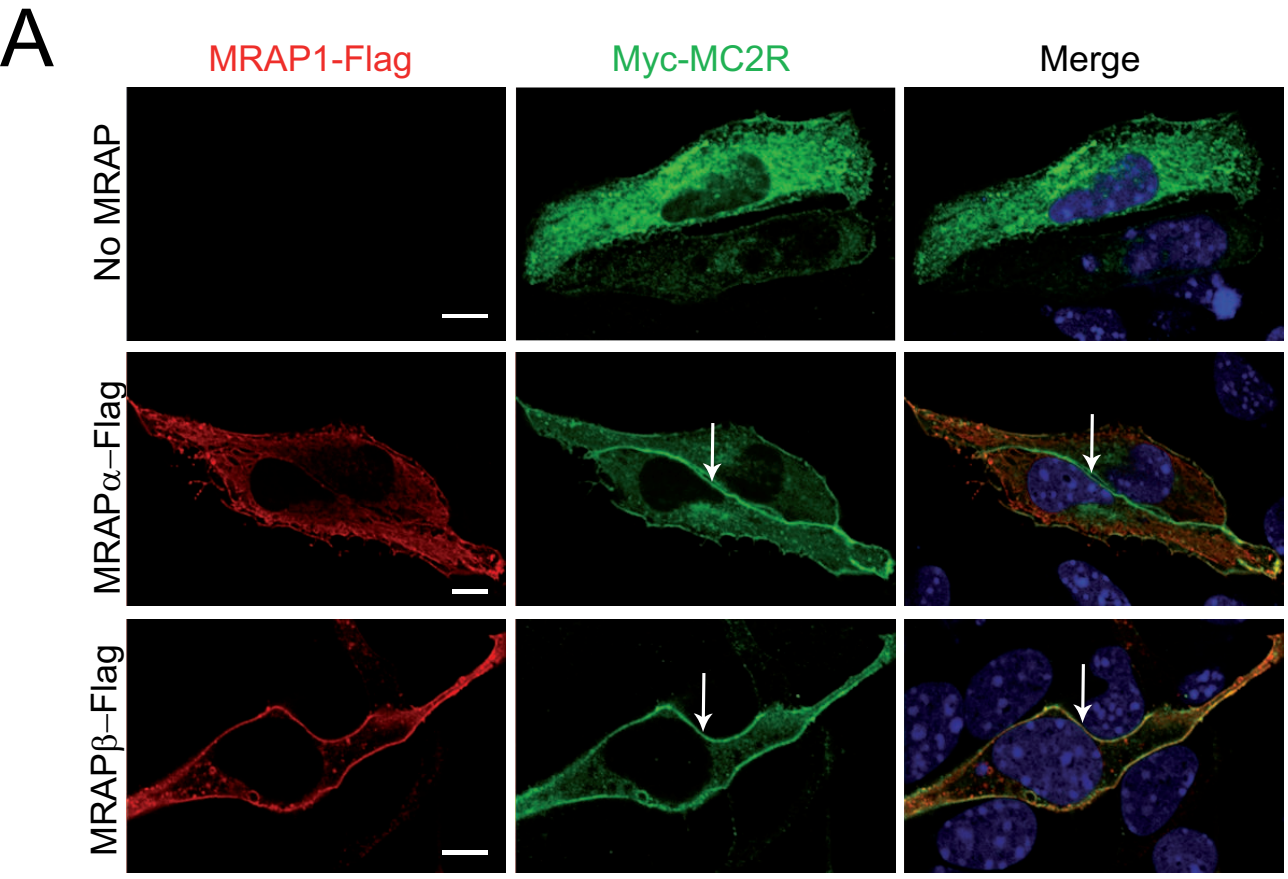
A
MRAP1-Flag
Myc-MC2R
Merge
No MRAP
MRAPα–Flag
MRAPβ–Flag

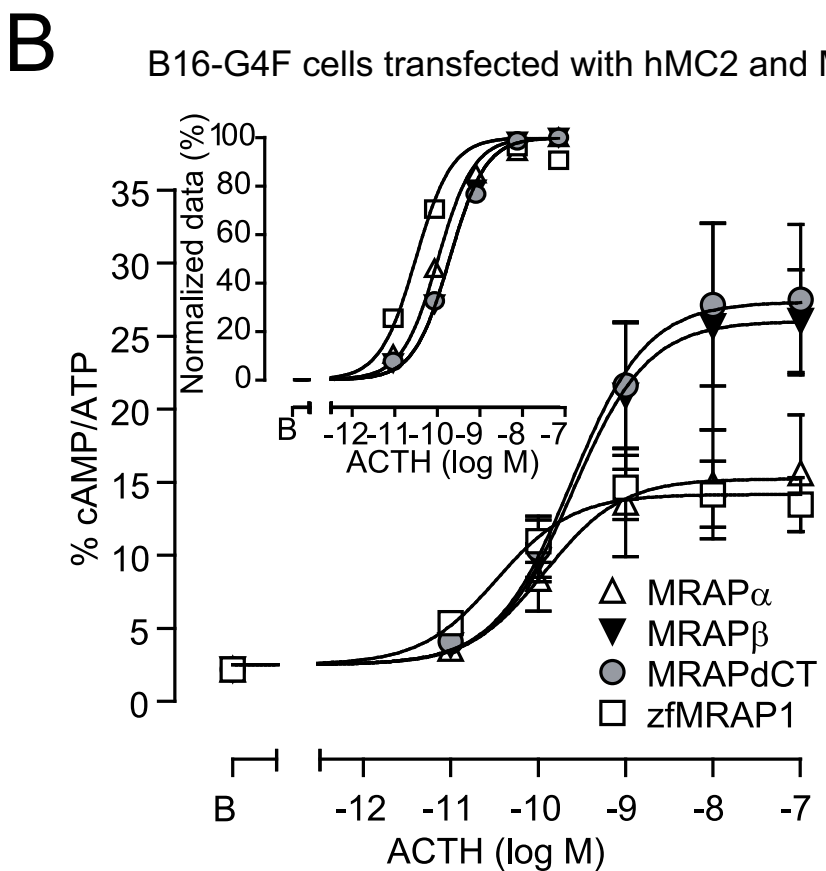
B
B16-G4F cells transfected with hMC2 and MRAP
% cAMP/ATP
Normalized data (%)
ACTH (log M)
B
-12 -11 -10 -9 -8 -7
MRAPα
MRAPβ
MRAPdCT
zfMRAP1